CLICdp-Conf-2016-006
10 June 2016

CLIC PHYSICS OVERVIEW

I. Božović-Jelisavčić[1)*]

On behalf of the CLICdp collaboration

[*] *Vinca Institute of Nuclear Sciences, University of Belgrade, Serbia*

Abstract

This paper, based on the invited talk given at the 17th Lomonosov Conference of Elementary Particle Physics, summarizes the physics program at CLIC, with particular emphasis on the Higgs physics studies. The physics reach of CLIC operating in three energy stages, at 350 GeV, 1.4 TeV and 3 TeV center-of-mass energies is reviewed. The energy-staged approach is motivated by the high-precision physics measurements in the Higgs and top sector as well as by direct and indirect searches for beyond the Standard Model physics. The first stage, at or above 350 GeV, gives access to precision Higgs physics through the Higgsstrahlung and WW-fusion production processes, providing absolute values of the Higgs couplings to fermions and bosons. This stage also addresses precision top physics around the top-pair-production threshold. The second stage, at 1.4 TeV, opens the energy frontier, allowing for the discovery of new physics phenomena. This stage also gives access to additional Higgs properties, such as the top-Yukawa coupling, the Higgs potential and rare Higgs decay branching ratios. The ultimate CLIC energy of 3 TeV enlarges the CLIC physics potential even further, covering the complete scope for precision Standard Model physics, direct searches for pair-production of new particles up to 1.5 TeV mass-scale, and provides the highest sensitivity to new physics models at much larger mass-scales through indirect searches. The staged implementation of CLIC would enable a long-term physics program at the energy frontier, providing insight into a wide range of physics measurements also beyond the capabilities of LHC and its high-luminosity upgrade.

17th Lomonosov Conference of Elementary Particle Physics, Moscow, 20–26 August, 2015, – special issue of the International Journal of Modern Physics A

[1)] ibozovic@vinca.rs

CLIC PHYSICS OVERVIEW

Ivanka Božović-Jelisavčić[a] on behalf of the CLICdp collaboration
Vinca Institute of Nuclear Sciences, University of Belgrade 11000 Belgrade, Serbia

Abstract. This paper, based on the invited talk given at the 17th Lomonosov Conference of Elementary Particle Physics, summarizes the physics program at CLIC, with particular emphasis on the Higgs physics studies. The physics reach of CLIC operating in three energy stages, at 350 GeV, 1.4 TeV and 3 TeV center-of-mass energies is reviewed. The energy-staged approach is motivated by the high-precision physics measurements in the Higgs and top sector as well as by direct and indirect searches for beyond the Standard Model physics. The first stage, at or above 350 GeV, gives access to precision Higgs physics through the Higgsstrahlung and WW-fusion production processes, providing absolute values of the Higgs couplings to fermions and bosons. This stage also addresses precision top physics around the top-pair-production threshold. The second stage, at 1.4 TeV, opens the energy frontier, allowing for the discovery of new physics phenomena. This stage also gives access to additional Higgs properties, such as the top-Yukawa coupling, the Higgs potential and rare Higgs decay branching ratios. The ultimate CLIC energy of 3 TeV enlarges the CLIC physics potential even further, covering the complete scope for precision Standard Model physics, direct searches for pair-production of new particles up to 1.5 TeV mass-scale, and provides the highest sensitivity to new physics models at much larger mass-scales through indirect searches. The staged implementation of CLIC would enable a long-term physics program at the energy frontier, providing insight into a wide range of physics measurements also beyond the capabilities of LHC and its high-luminosity upgrade.

1 Introduction

Future Compact Linear Collider (CLIC) offers excellent potential for precision measurements in the QCD clean environment of e^+e^- collisions. Over the last years, the feasibility studies for the CLIC accelerator and detector have addressed the main technical challenges of the accelerator and detector projects [1], [2].

1.1 CLIC accelerator and detector

The CLIC project is based on a novel two-beam acceleration scheme, where a high-intensity beam (drive beam) is used to generate RF power to the main beam. Using normal-conducting accelerator structures, the two-beam acceleration provides gradients of 100 MV/m as has been demonstrated at the CTF3 test facility [1]. The machine is foreseen to run at three center-of-mass energies assuming 350 GeV, 1.4 TeV and 3 TeV, re-using the existing equipment for each new stage. The assumed integrated luminosities of 0.5 ab^{-1} at 350 GeV, 1.5 ab^{-1} at 1.4 TeV and 2.0 ab^{-1} at 3 TeV correspond to four years of operation at each stage, for a fully commissioned machine running 200 days per year with an effective up-time of 50%. The CLIC design foresees 80% electron polarization, while positron polarization is an option.

Small (σ_x=40 nm, σ_y=1 nm) and dense ($\sim 10^9$ particles) bunches, essential for obtaining high luminosity, result also in a strong beamstrahlung induced by the electromagnetic fields of the opposite bunches. Consequently, 3.2 interactions of the

[a]E-mail: ibozovic@vinca.rs

beamstrahlung photons producing hadrons are expected per bunch-crossing at 3 TeV center-of-mass energy. With a small bunch separation of 0.5 ns, the time-stamping of 10 ns is required, in order to cope with the occupancy of the central detectors. The effect of time-stamping on suppression of hadronic background from beamstrahlung ($\gamma_{BS}\gamma_{BS} \rightarrow hadrons$) is illustrated in Figure 1. In addition, particle-flow algorithm (PFA) used for event reconstruction [3] provides a powerful tool for the rejection of beam-induced background [1]. Altough beamstrahlung severely deteriorates luminosity spectrum, in particular at high center-of-mass energies, it has been shown that this effect can be controlled at a permille level in the peak region above the 80% of the nominal center-of-mass energies [4].

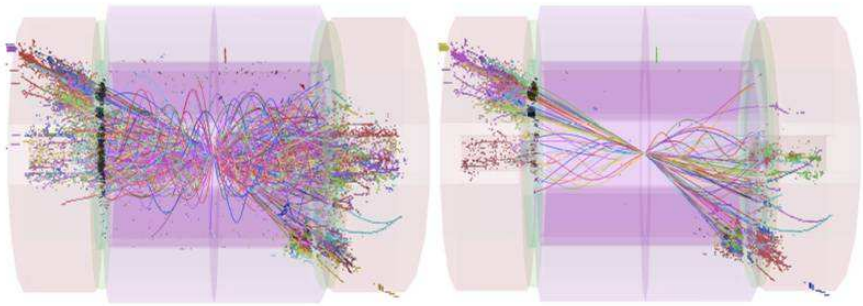

Figure 1: Reconstruction of the $t\bar{t}$ event with overlaid background from beamstrahlung ($\gamma_{BS}\gamma_{BS} \rightarrow hadrons$), at 3 TeV CLIC, before (left) and after (right) applied time-stamping.

CLIC_SiD [5] and CLIC_ILD [6] detector concepts were used in the CLIC analyses presented in this paper. Both concepts, optimized to the CLIC running conditions, have been recently merged into the CLICdet_2015 detector model currently being under development based on the software package DD4hep [7]. Detector performance is driven by the physics goals requiring:

- jet energy resolution for high-energy jets above 100 GeV better than 3.5%,
- track momentum resolution $\sigma_{p_T}/{p_T}^2 \sim 10^{-5}$ GeV^{-1},
- impact parameter resolution of the order of a few microns.

Among others, the above requirements come from the need to distinguish between Z, W or Higgs bosons from the jet invariant mass measurement, to reconstruct the Higgs boson from the recoil mass of the Z decay products (i.e. muons) and to provide the flavor separation as in the measurement of the Higgs couplings to beauty and charm. Detector hermeticity, with the very forward electron tagging down to 10 mrad and high lepton identification efficiency (over 95%) is assumed at all energy stages. In Figure 2 [8], a schematic view of the CLICdet_2015 detector model is given.

It comprises the ultra low-mass vertex detector with 0.2% X_0 material budget per layer, all-silicon tracker motivated by very high TPC occupancy at 3 TeV, fine grained calorimetry to enable best PFA performance on particle identification and kinematic reconstruction based on the combined tracker and calorimetry information [8], and extended all-silicon tracker coverage motivated by the forward region measurements (i.e. Higgs self-coupling). The full coverage is also important to suppress Standard Model (SM) backgrounds in various physics analyses.

CLIC beams will arrive at the detector in bunch trains, occurring every 20 ms. Each bunch train gives 312 bunch crossings at 0.5 ns time separation (at 3 TeV center-of-mass energy). This time structure allows for a triggerless readout of the detectors after each bunch train. It also allows for a power-pulsing scheme for the powering of the detector electronics, thereby significantly reducing the power dissipation and the tracker mass. On average, less than one physics event per bunch train is expected.

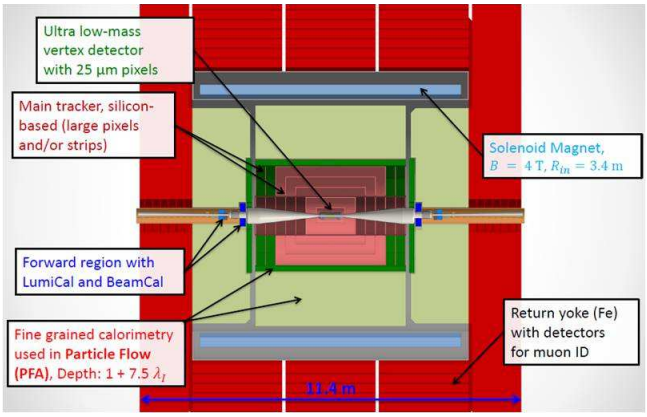

Figure 2: Longitudinal cross-section of the CLICdet_2015 detector model.

1.2 Overview of the CLIC physics program

CLIC is foreseen as an energy-staged machine motivated by the high-precision physics measurements in the Higgs and top sector as well as by beyond the Standard Model (BSM) searches through direct and indirect measurements. Illustration of the staging scenario to address various physics processes of interest is given in Figure 3 [9], where cross-sections are given versus the available center-of-mass energy.

The first stage, at or above 350 GeV, gives access to precision Higgs physics through the Higgsstrahlung ($e^+e^- \to HZ$) and WW-fusion production processes ($e^+e^- \to H\nu_e\bar{\nu}_e$), providing absolute values of Higgs couplings to both fermions and bosons. This stage also addresses precision top physics around the top-pair production threshold ($e^+e^- \to t\bar{t}$).

The second stage, around 1.4 TeV, opens possibility to directly produce new particles e.g. charginos, squarks, neutralinos. This stage also gives access to additional Higgs properties, such as the top Yukawa coupling, the Higgs potential and rare Higgs decay branching ratios.

The ultimate CLIC energy of 3 TeV enlarges the CLIC physics potential even further, covering the complete scope for precision Standard Model physics, allowing direct searches for pair-production of new particles up to 1.5 TeV mass and providing the highest sensitivity to new physics models through indirect searches.

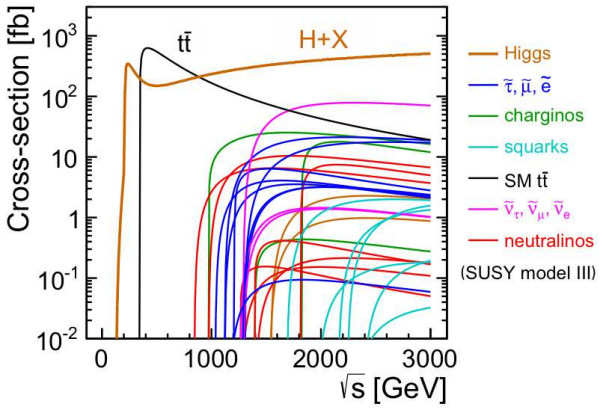

Figure 3: Higgs, top-pair and SUSY production cross-sections in the SUSY model III [10], as a function of the center-of-mass energy. Every line of a given color corresponds to the production cross-section of one particle in the legend.

2 Higgs studies

The discovery of a Higgs boson at the LHC [11], [12] provided confirmation of the electroweak symmetry breaking mechanism, leaving the open questions such as if the observed Higgs boson is the fundamental singlet scalar of the Standard Model or it is either a more complex object, or a part of an extended Higgs sector. Being the Higgs factory, with an overall statistics of $\sim 10^6$ Higgs bosons from all energy stages, (assuming four years of nominal detector operation per stage), the CLIC offers excellent possibilities for precision measurements of the Higgs properties.

Higgsstrahlung and WW-fusion are the dominant production mechanisms of the Higgs boson at low and high energies, respectively (Figure 4 a) and b)). In addition, ZZ-fusion gives non-negligible contribution to the Higgs production at high energies (Fugure 4 c)). Depending on the production mechanism, appropriate polarization could eventually double the statistics. The impact of the electron (positron) polarization for various Higgs production mechanisms is given in Table 1 [9]. The expected

number of Higgs bosons produced per energy stage, with unpolarized beams, is given in Table 2 [9], while Figure 5 illustrates the cross-section dependence on the available center-of-mass energies for various Higgs production mechanisms.

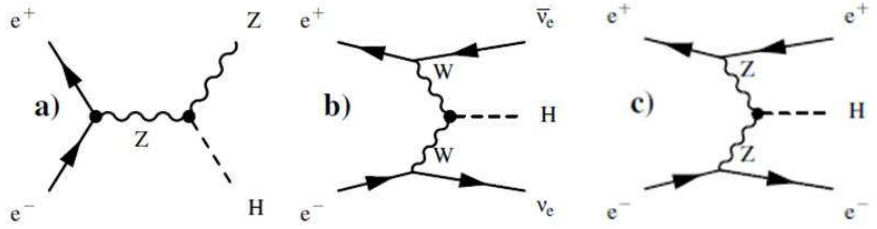

Figure 4: Feynman diagrams of the Higgsstrahluing (a) ,WW-fusion (b) and ZZ-fusion (c), the leading-order processes to produce Higgs bosons at low and high energies, respectively.

Polarisation	Enhancement factor	
$P(e^-) : P(e^+)$	$e^+e^- \to ZH$	$e^+e^- \to H\nu_e\bar{\nu}_e$
unpolarised	1.00	1.00
-80% 0%	1.12	1.80
$-80\% +30\%$	1.40	2.34
$-80\% -30\%$	0.83	1.26

Table 1: The dependence of the event rates for the Higgsstrahlung, WW-fusion and ZZ-fusion respectively, for several examples of beam polarizations.

$\sqrt{s} =$	350 GeV	1.4 TeV	3 TeV
$\mathscr{L}_{\text{int}}$	500 fb^{-1}	1500 fb^{-1}	2000 fb^{-1}
$\sigma(e^+e^- \to ZH)$	134 fb	9 fb	2 fb
$\sigma(e^+e^- \to H\nu_e\bar{\nu}_e)$	52 fb	279 fb	479 fb
$\sigma(e^+e^- \to He^+e^-)$	7 fb	28 fb	49 fb
$\#ZH$ events	68,000	20,000	11,000
$\#H\nu_e\bar{\nu}_e$ events	26,000	370,000	830,000
$\#He^+e^-$ events	3,700	37,000	84,000

Table 2: Assumed integrated luminosities, the leading-order unpolarized Higgs production cross-sections and the expected numbers of events for the Higgsstrahlung, WW-fusion and ZZ-fusion processes, for simulated Higgs mass of 126 GeV, at the three centre-of-mass energies.

Combined study of the Higgsstrahlung and WW-fusion can be used to probe the Higgs width and couplings in a model-independent way. This leads to a determination

of the Higgs couplings at the level of $\sim$1% (except for the rare decays to light particles such as muons or photons). Assuming that the Higgs total width is constrained by the SM decays, the statistical precision of the Higgs couplings can be improved to the sub-percent level. Details of the Higgs measurements at low and high-energy stages, and the combined fit will be discussed in Section 2.1 and 2.2.

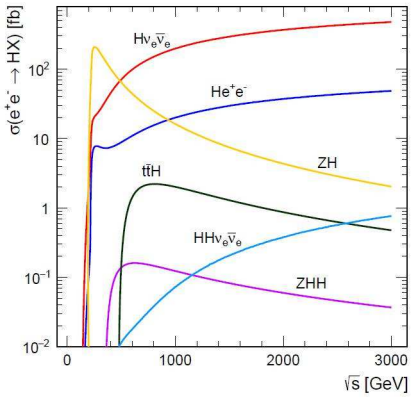

Figure 5: Cross-section dependence on the available center-of-mass energies for various Higgs production final states.

2.1 Low and high-energy landscape

From the perspective of the Higgs studies, the low-energy phase of CLIC is primarily motivated by the direct and model-independent measurement of the Higgs coupling to Z boson (g_{HZZ}). It can be obtained from the recoil mass distribution in Higgsstrahnlung ($e^+e^- \to ZH, Z \to f\bar{f}, f = e, \mu, q$) with a statistical precision of 0.8% [13]. The g_{HZZ} determination plays a central role in the model-independent determination of the Higgs couplings. Using the Z decays to leptons, recoil mass distribution can be used to extract the Higgs mass and the total ZH production cross-section with the statistical precision of 120 MeV and 4% [9], respectively. Limitations of these measurements come from the small branching ratios for leptonic Z boson decay channels and the impact of the CLIC beamstrahlung spectrum producing a tail in the recoil mass distribution, as illustrated in Figure 6 (left). For hadronic Z decays, the recoil mass distribution allows for a direct search for invisible Higgs decays, constraining the branching ratio for $H \to$ *invisible* decays to 0.90% at 95% CL [14]. In Figure (Figure 6 (right)) recoil mass distribution for $HZ, Z \to q\bar{q}$ signal is given against the $q\bar{q}$ invariant mass [14].

In general, at 350 GeV center-of-mass energy, the main Standard Model background processes are two- and four-fermion production, while at higher energy stages background from hard interactions of beamstrahlung photon ($\gamma_{BS}\gamma_{BS}$ and $\gamma_{BS}e^{\pm}$) be-

comes relevant for the Higgs related measurements, as well. Additionally, soft $\gamma_{BS}\gamma_{BS} \rightarrow$ *hadrons* events pile-up with the hard interaction events of interest. However, this background of relatively low-p_T particles can be significantly reduced through timing cuts and preselecton. In all the CLIC Higgs analyses, the full list of beam-induced and physics backgrounds is considered and optimally reduced (w.r.t. the signal) through preselection and multivariate analyses (MVA) used as the signal selection steps.

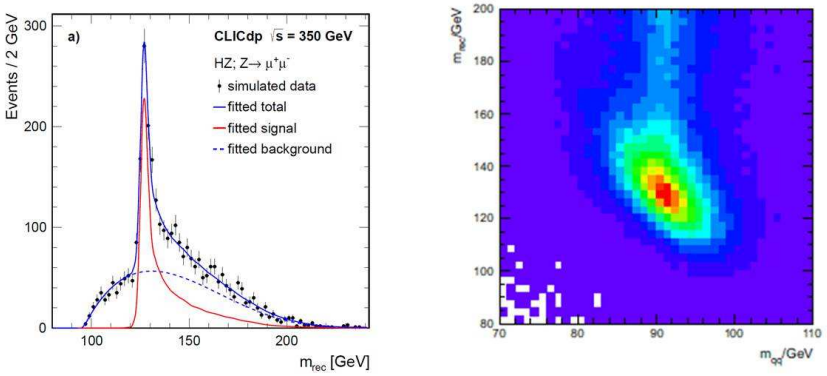

Figure 6: Recoil mass distribution from $HZ, Z \rightarrow \mu^+\mu^-$ decays, at 350 GeV center-of-mass energy. The plot is normalized to the integral luminosity of 500 fb^{-1} (left). Recoil mass is given against $q\bar{q}$ invariant mass, for $HZ, Z \rightarrow q\bar{q}$ decays at 350 GeV center-of-mass energy (right).

With a cross-section σ_{Hvv} scaling as $log(s)$, WW-fusion becomes the dominant Higgs production channel at higher energies. The golden channel $H \rightarrow b\bar{b}$ can be exploited for the Higgs mass measurement, resulting in the statistical precision $\Delta(m_H) = \pm$ 30 MeV achievable at higher energies [9]. Illustration of the Higgs mass distribution reconstructed from the two b-jets at 3 TeV center-of-mass energy, in the presence of the Standard Model background, is given in Figure 7 [13].

The high Higgs production cross-section in WW fusion allows to probe rare decays (BR $\leq 10^{-3}$) like $H \rightarrow \mu^+\mu^-$, $H \rightarrow Z\gamma$ and $H \rightarrow \gamma\gamma$ already at 1.4 TeV, with a statistical precision of 38%, 42% and 15% respectively [13]. These numbers scale down by a factor $\sim$0.7 if electron polarization of 80% is applied. Further gain in precision can be achieved at 3 TeV center-of-mass energy, where the Higgs production cross-section is approximately 70% higher than at 1.4 TeV. For example, at 3 TeV center-of-mass energy, $H \rightarrow \mu^+\mu^-$ decay can be measured with a relative statistical uncertainty on $\delta(\sigma_{Hvv} \cdot BR(H \rightarrow \mu^+\mu^-))$ of 19.2% [15]. In Figure 8, expected distributions of the reconstructed di-muon and di-photon invariant masses are shown, for $H \rightarrow \mu^+\mu^-$ decays (left) [15] and $H \rightarrow \gamma\gamma$ decays (right) [16], at 1.4 TeV center-of-mass energy. The main limitation in the achievable precision in rare Higgs decays measurements comes from the signal statistics and irreducible Standard Model background processes (with the same final state as the signal). This is illustrated in Figure 9 [13], where the mul-

tivariate approach has been employed to optimally separate between the signal and numerous background procesess with different kinematics.

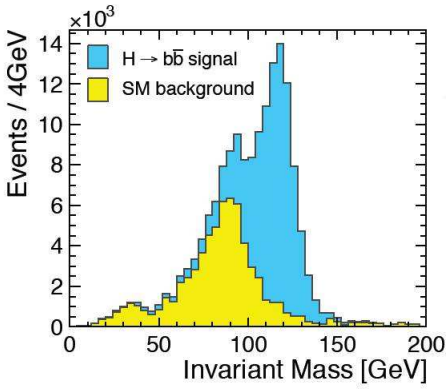

Figure 7: Di-jet invariant mass reconstructed for $H \to b\bar{b}$ decays and the corresponding SM background, at 3 TeV center-of-mass energy, normalized to the integral luminosity of 2 ab^{-1}.

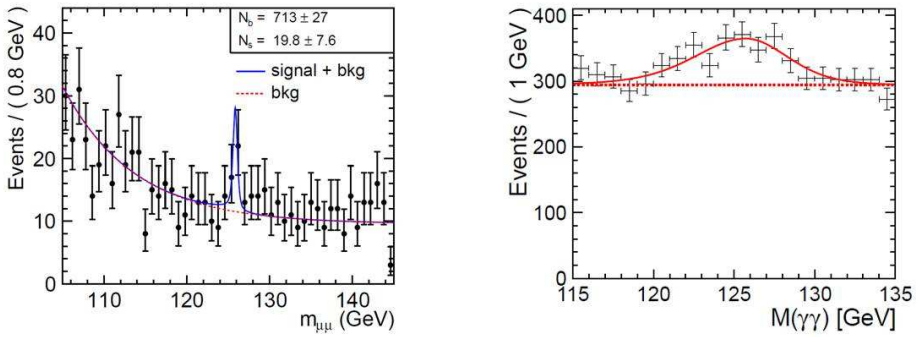

Figure 8: Reconstructed di-muon invariant mass in $H \to \mu^+\mu^-$ decays at 1.4 TeV center-of-mass-energy (left). Reconstructed di-photon invariant mass in $H \to \gamma\gamma$ decays at 1.4 TeV (right). Distributions are normalized to the integral luminosity of 1.5 ab^{-1}.

Excellent performance of tagging algorithms allows heavy flavor separation and the corresponding statistical uncertainty to access $\sigma_{H\nu\nu} \cdot BR(H \to b,c,g)$ at 3 TeV center-of-mass energy is 0.2%, 2.7% and 1.8% [13], respectively (for the Higgs decays to b, c and gluons), yielding a statistical precision of 1.5% on the ratio g_{Hcc}/g_{Hbb} [9]. The latter provides a direct test of the Standard Model predictions for the up and down-type of quarks. In Figure 10 [1], flavor-tagging separation power is illustrated for 3 TeV CLIC.

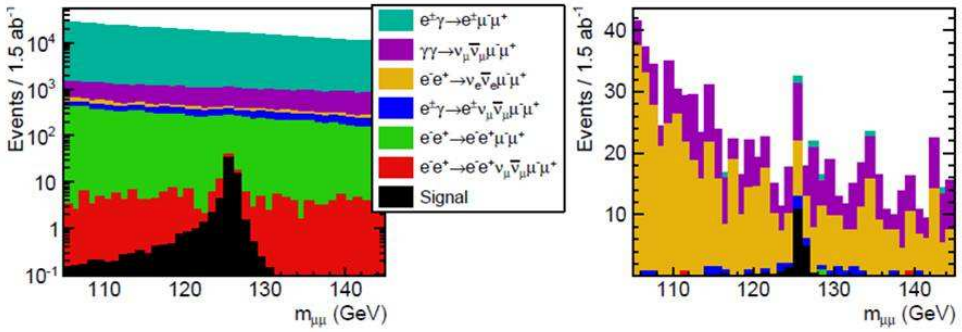

Figure 9: Reconstructed Higgs invariant mass distribution for $H \to \mu^+\mu^-$ events at 1.4 TeV, showing the signal and main background as stacked histograms: left) after preselection, and right) after the full event selection including MVA. Distributions are normalized to the integral luminosity of 1.5ab^{-1}.

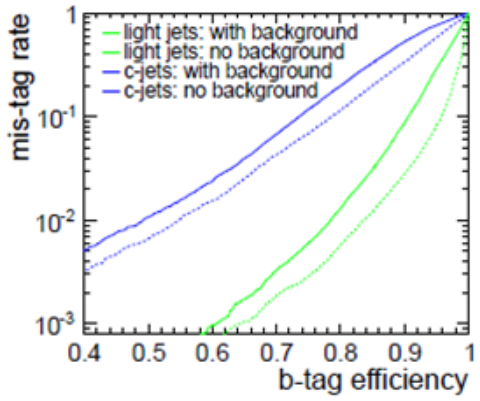

Figure 10: Flavor-tagging separation of heavy quarks at 3 TeV CLIC.

Particular relevance of the high energy running lies in the ability to access the Higgs self-coupling λ and quartic coupling to W bosons (g_{HHWW}) in a double-Higgs production via WW-fusion ($e^+e^- \to HH\nu_e\bar{\nu}_e$), as illustrated in Figure 11 a) and b), respectively.

The double-Higgs production cross-section is sensitive to the trilinear Higgs self-coupling λ that determines the shape of the fundamental Higgs potential. Since not only the λ-sensitive diagram (Figure 11 a)) contributes to the double-Higgs production, effect of other processes must also be taken into consideration. That can be done either through generator-based parameterization of the $HH\nu\bar{\nu}$ cross-section as a function of the input value for λ (Figure 12), or by fitting the neural network out-

put distribution with the Monte Carlo templates of double-Higgs events including the λ-sensitive Feynman diagram for various assumptions on λ together with the other contributing processes. The latter method is preferable, as the first method does not account for the possibility that the event selection might favor some Feynman diagrams over others. The cross-section illustrated in Figure 12 [17] is then used as a cross check.

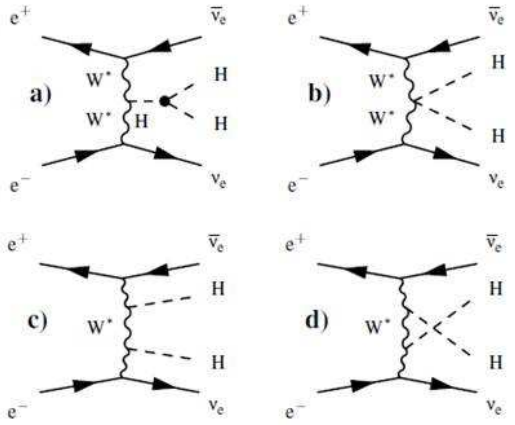

Figure 11: Feynman diagrams of the leading-order processes (a,b,c,d) that produce two Higgs bosons and missing energy at CLIC above 1 TeV center-of-mass energies. The diagram (a) is sensitive to the trilinear Higgs self-coupling λ. The diagram (b) is sensitive to the quartic coupling g_{HHWW}.

Despite the small cross-section for double-Higgs production at 1.4 TeV and 3 TeV center-of-mass energies (0.15 fb and 0.59 fb respectively), the Higgs boson trilinear coupling parameter λ can be extracted with a relative statistical uncertainty of 12%, assuming electron beam polarization of -80% [17]. Beam polarization plays an important role in this type of measurements due to the increase of the Higgs production cross-section and the suppression of certain types of background (Table 1). Combination of both high-energy stages improves the statistical precision on λ by a few percent.

In addition, double Higgs production provides the potential to extract the quartic g_{HHWW} coupling using a dominant process that occurs when both Higgs bosons decay to b-quarks, resulting in four b-jets and missing momentum signature. The quartic g_{HHWW} coupling can be extracted with a relative statistical uncertainty of 3% at 3 TeV CLIC [13].

2.2 Combined fit of the Higgs measurements

The full statistics of data (0.5 ab^{-1} at 350 GeV, 1.5 ab^{-1} at 1.4 TeV, 2 ab^{-1} at 3 TeV) can be used in a global fit in order to reach the ultimate precision on the Higgs cou-

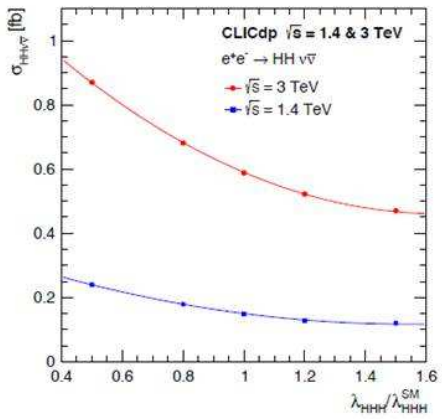

Figure 12: Cross-section for the double-Higgs production at 1.4 TeV and 3 TeV as a function of the Higgs self-coupling ratio w.r.t. the Standard Model value ($\lambda/\,\lambda_{SM}$).

plings. Direct access to g_{HZZ}, through Higgstrahlung at the lowest center-of-mass energy, allows a fit with minimal theoretical assumptions where the Higgs couplings and the Higgs total width enter as free parameters. For each production and decay chanell, measured $\sigma \times BR$ can be related to the corresponding coupling combination, e.g. for $\sigma(e^+e^- \to HZ) \times BR(H \to b\bar{b})$:

$$C_{HZ,H\to b\bar{b}} = \frac{{g_{HZZ}}^2 \cdot {g_{Hbb}}^2}{\Gamma_H} \tag{1}$$

and, similarly for other processes. Then, the overall χ^2 can be built:

$$\chi^2 = \sum_{i=1,10} \frac{(C_i/C_i^{mod} - 1)^2}{{\delta F_i}^2} \tag{2}$$

where C_i^{mod} is the model expectation for C_i, and δF_i stands for the relative statistical uncertainty of the $\sigma \cdot BR$ observable for the considered Higgs decay i. Relative uncertainty of the Higgs production cross section times the branching ratio ($\sigma \cdot BR$) of a givven process i is equivalent to the uncertainty of C for that process (C_i).

The above leads to the determination of the Higgs total width with a relative statistical uncertainty of 3.5% at 3 TeV CLIC [13], while most of the couplings can be determined at a percent level. The uncertainties are slightly higher for the rare Higgs decays to $\mu^+\mu^-$, $Z\gamma$ and $\gamma\gamma$ as shown in [9].

On the other hand, assuming that the total (model-dependent) width is determined from the Standard Model branching ratios, a global fit can be performed in a model-

dependent way, with the relative partial widths κ_i (i=1,9) as free parameters:

$$\Gamma_H^{md} = \sum_{i=1,9} \kappa_i^2 BR_i^{SM} \qquad\qquad \kappa_i^2 = \Gamma_i/\Gamma_i^{SM} \tag{3}$$

Then, instead of couplings, the corresponding relative partial widths can be used to define fitted values e.g. :

$$C_{HZ,H\to b\bar{b}} = \frac{\kappa_{HZZ}^2 \cdot \kappa_{Hbb}^2}{\Gamma_H^{md}} \tag{4}$$

The above, LHC-style approach, leads to a sub-percent precision for most of the couplings, as indicated in [9]. Results presented in [9] have been improved through the refinement and completion of the on-going Higgs analyses, and are to be published soon as a CLIC Higgs physics summary paper. Each of the stages contributes significantly to the total precision, where the first stage at 350 GeV provides the model-independent measurement of the Higgs to Z coupling to which all the other coupling measurements will be correlated to. The higher-energy stages add direct measurements of the couplings to top quark (that will be discussed in Section 3), to muons and photons, as well as the overall improvement of the Higgs couplings measurements except for the one to the Z boson, already measured in the first stage.

In Figure 13 [9], Higgs couplings and their uncertainties, measured above 1 TeV assuming -80% electron beam polarization, are given as illustration of a test of the coupling-mass linearity predicted by the Standard model.

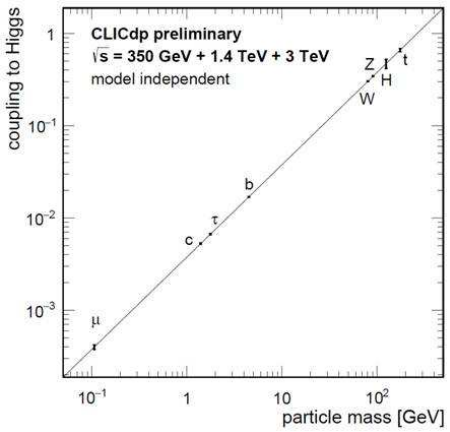

Figure 13: Illustration of the CLIC results on the Higgs couplings, above 1 TeV center-of-mass energies and with -80% beam polarization, as a test of the coupling-mass linearity predicted by the Standard Model.

3 Top studies

Due to its high mass, the top-quark provides leading contributions to higher order corrections in many processes that can be sensitive to physics beyond the Standard Model. Also, together with the Higgs mass, the top mass is a key input to studies of the vacuum stability of the Standard Model. With the current precision of the Higgs mass provided by the LHC, the uncertainty of the top mass is the leading uncertainty in this evaluation. Improved measurement of the top-quark mass, possible at a linear collider, will substantially reduce LHC (CMS) current uncertainties of the top mass $m_t = 172.44 \pm 0.13 \pm 0.47$ GeV [18]. This is due to the easier reconstruction of the final state at a lepton collider, as well as to the fact that the theoretical uncertainties are significantly smaller than at LHC.

The CLIC offers two complementary ways of the top mass measurement. One is by direct reconstruction of the invariant mass of the top decay products, which can be performed at arbitrary center-of-mass energy, and the other is based on the cross-section scan around the top-pair production threshold. The latter requires higher-order theoretical corrections to be taken into account. The invariant mass approach leads to the top mass statistical uncertainty of 80 MeV at 500 GeV, while the threshold scan provides 30 MeV statistical uncertainty, for the same total integrated luminosity of $100\,\text{fb}^{-1}$. The total error from treshold scan of 100 MeV is dominated by the theoretical uncertainty. In Figure 14 [19], top mass direct reconstruction (left) and the top threshold scan (right) are illustrated for a 174 GeV simulated top mass.

At an e^+e^- collider, the top Yukawa coupling can be determined from the event rate in the process where a Higgs boson is produced in association with a top-quark pair, $(e^+e^- \to t\bar{t}H)$. The top quarks decay almost exclusively to bW, so the event topology depends on the nature of the W and Higgs boson decays. In either fully hadronic (both W decays hadronically) or semi-leptonic case (one W decays leptonically), event reconstruction is demanding due to a multi-jet topology (illustrated in Figure 15). The jets are combined to form candidates of primary particles (t, W and Higgs) in a way to minimize a χ^2 function describing the consistency of the reconstructed tri-jet and di-jet invariant masses.

Excellent flavor tagging as well as the possibility to separate between hadronic W and H decays based on the di-jet invariant masses enables measurement of the top Yukawa coupling at 1.4 TeV center-of-mass energy. With electron polarization of -80%, it is possible to achieve relative statistical uncertainty of the top Yukawa coupling below 4%. Since the cross-section for the $t\bar{t}H$ production falls with increasing center-of-mass energy, the precision at 3 TeV is not expected to be better than the result at 1.4 TeV.

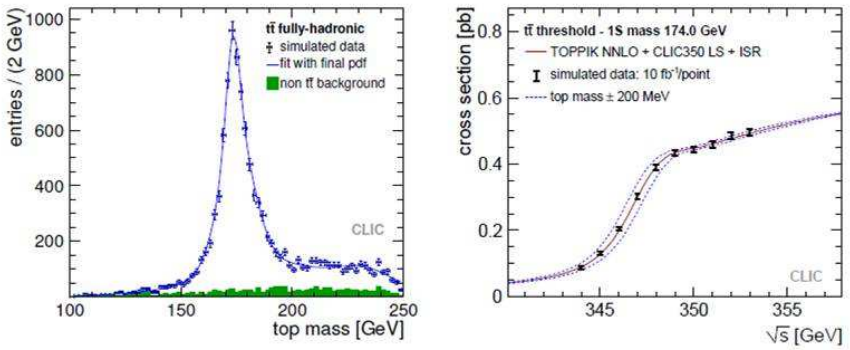

Figure 14: Reconstructed top-quark mass in the all-hadronic decay channel for an integrated luminosity of 100 fb^{-1} at 500 GeV. The top mass and width are determined with an unbinned maximum likelihood fit to the invariant mass distribution, shown by the solid line (left). Illustration of a scan of the top-quark pair production threshold, with each point corresponding to 10 fb^{-1} of integrated luminosity (right). The sensitivity to the top quark mass is illustrated by showing the top pair production cross-section for 200 MeV changes in the top mass.

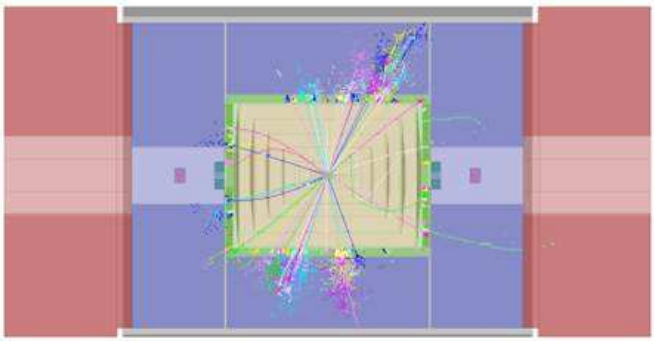

Figure 15: Event display of a 6-jet event $t\bar{t}H \to b\bar{b}b\bar{b}q\bar{q}\tau^{-}\bar{\nu}_{\tau}$ at 1.4 TeV center-of-mass energy in the CLIC_SiD detector. The tau lepton decays hadronically.

4 BSM searches

The fact that the Standard Model of particle physics is an mathematically open theory, as well as the existing questions that cannot be addressed within it, like the quest for a dark matter candidate, baryon asymmetry of the universe, CP violation, eventual unification of fundamental interactions, stability of the SM vacuum, etc., give rise to a wide spectrum of theories that extend the Standard Model. The CLIC offers a possibility to test many of these theories with a reach going far beyond the capabil-

ities of LHC and HL-LHC as will be described in the following sections. Potential signatures of beyond the Standard Mode physics can be searched for either through direct reconstruction of new particles, with an approximate mass reach of $\sim 1/2\sqrt{s}$, or indirectly, by searching for (model dependent) deviations in precision observables (like cross-sections, FB and LR asymmetries, etc.). Some prominent examples will be given in the following sections 4.1 through 4.3, while the complementarities with the LHC and HL-LHC program will be discussed in section 4.4.

4.1 Supersymmetry

Supersymmetry is a very well motivated theory featuring a natural dark matter candidate, a possible unification of the forces at high energies, and having the ability to solve the electroweak scale hierarchy problem. However, results of the LHC Run I have ruled out the existence of most of the superpartners, up to the mass scale of 1.8 TeV with 95% CL [20]. Supersymmetry is necessarily (at least) a Two-Higgs-Doublet theory, and a full test of its underlying structure requires measuring the four heavier Higgs bosons, $H^{\pm}$, A and H. As illustrated in Figure 16 [13], the CLIC has the ability to measure these masses to a percent level and to distinguish the mass splitting among all of these states, what can be crucial for understanding of the underlying model. It should be noted that models with two Higgs doublets (2HDM) are not necessarily restricted to supersymmetry. Particles under consideration can be just described as states with given mass, spin and quantum numbers. Performed studies serve as an illustration of CLIC capabilities, independently of a new physics model.

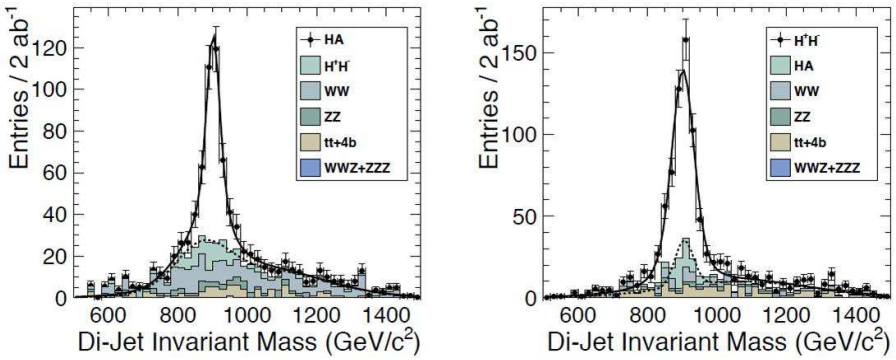

Figure 16: Di-jet invariant mass distributions for Model I [1], for $b\bar{b}, \bar{b}b$ forming HA states (left) and $t\bar{b}, b\bar{t}$ forming H^+H^- states (right), at 3 TeV CLIC. The CLIC_ILD detector is fully simulated assuming the integrated luminosity of 2 ab^{-1}.

In principle, direct searches provide sensitivity to the mass range of $\sim 1/2\sqrt{s}$, that can be determined at a percent level, assuming range of masses of $\approx$ 350 GeV for

the lightest neutralino, $\approx$ 480 - 650 GeV for heavier neutralinos (charginos), approximately 550 GeV - 1.1 TeV for charged sleptons, and $\approx$ 1.1 TeV for light-flavored squarks, depending on a SUSY model (Model I, II, III [1]). Final state particles energy spectrum, such as W bosons or muons from $e^+e^- \to \widetilde{\chi}_1^+\widetilde{\chi}_1^- \to W^+W^-\widetilde{\chi}_1^0\widetilde{\chi}_1^0$ or $e^+e^- \to \widetilde{\mu}_R^+\widetilde{\mu}_R^- \to \mu^+\mu^-\widetilde{\chi}_1^0\widetilde{\chi}_1^0$ can be used to measure masses of $\widetilde{\chi}_1^\pm$ or $\widetilde{\mu}_1^\pm$, as well as of neutralino (LSP). Ideal "box shape" energy distribution as shown in Figure 17 [21], is distorted by the luminosity spectrum giving the systematic contribution to the uncertainty of masses of about 40 MeV. For a smuon mass around 1 TeV and a 340 GeV neutralino mass, the statistical uncertainty in mass determination is of the order of 5-6 GeV at 3 TeV CLIC.

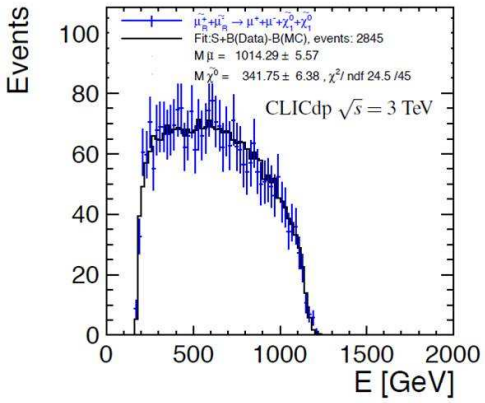

Figure 17: Muon energy spectrum expected from smuon production and decays at 3 TeV CLIC. End-points are used to determine smuon and neutralino masses.

Very good jet energy resolution is crucial for proper reconstruction of gaugino decays to Higgs, W or Z bosons enabling statistical precision at a percent level or better, achievable at 3 TeV CLIC . Illustration of gaugino event reconstruction for three possible decay channels is given in Figure 18 [22].

4.2 Higgs compositeness

The fact that scalar masses receive higher-order corrections resulting in a quadratic divergence of a scalar mass at a higher scale, remains an open question in the absence of supersymmetry. A BSM option that is not yet excluded by the current LHC data is that the Higgs boson is not a fundamental scalar, but rather a composite state of fermions. In that case, every observable receives relative correction to it that is proportional to $\xi = (\frac{v}{f})^2$, where $v \approx$246 GeV is the vacuum expectation value and $4\pi f$ is the scale of compositeness. Using the combined fit of single and double Higgs production, with 2 ab^{-1} of data at 3 TeV CLIC, it should be possible to exclude coupling

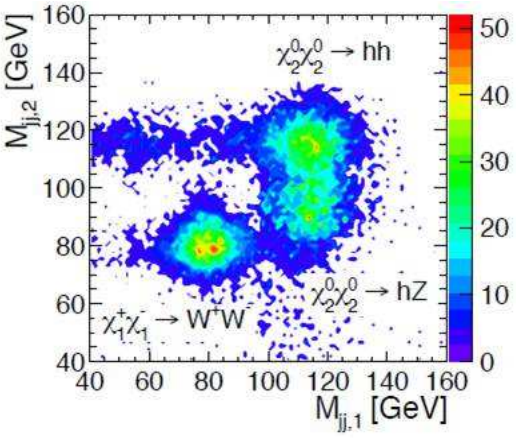

Figure 18: Gaugino event reconstruction at 3 TeV CLIC for different decay channels.

values down to $\xi \approx 0.002$ that corresponds to the scale of compositeness of 70 TeV. In Figure 19 [23], the reach in ξ is given for different experiments as a function of m_ρ, where ρ stands for the vector resonance of the composite theory.

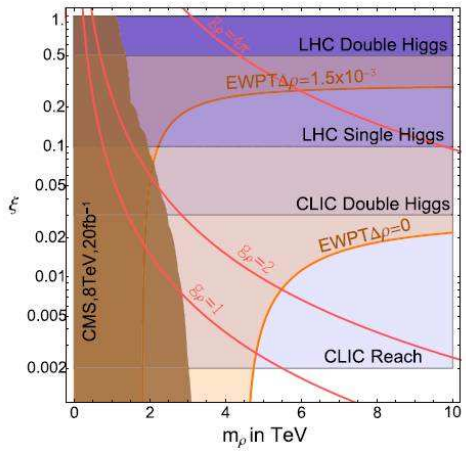

Figure 19: Summary plot of the current constraints on the Higgs compositeness from CLIC and LHC. 300 fb^{-1} of integrated luminosity is assumed for double (single) Higgs production at LHC. The 'CLIC Double Higgs' band corresponds to a double Higgs production alone, at 3 TeV CLIC with 1 ab^{-1} of integrated luminosity. The final CLIC reach includes the single Higgs production, in addition.

It is interesting to note that with an integrated luminosity of 1 ab^{-1} accumulated

at 3 TeV, CLIC can reach $\xi \approx 0.03$ independently of m_ρ, due to the relatively clean environment for studying double Higgs boson production in e^+e^- collisions. For comparison, the LHC running at 14 TeV center-of-mass energy, with an integrated luminosity of 300 fb^{-1} can reach only down to $\xi \approx 0.1$ (Figure 19).

4.3 Extended gauge theories

At e^+e^- colliders, and in particular at high energies, fermion pair-production can be used to probe higher order corrections coming from the extended gauge theories. The sensitive observables include the total cross-section, forward-backward asymmetry, and polarization asymmetries. As an example, sensitivity to a new Z bozon (Z') that couples to leptons in $e^+e^- \to \mu^+\mu^-$ is shown in Figure 20 [24]. Discovery limits (5σ intervals) of the Z' gauge boson mass are shown as a function of the integrated luminosity, assuming the measured cross-section and asymmetries are the considered observables. The sensitivity reaches masses of several tens of TeV (depending on the coupling assumptions), what is well beyond the available center-of-mass energy, and well beyond what the reach of LHC or its conceived upgrades (see Section 4.4).

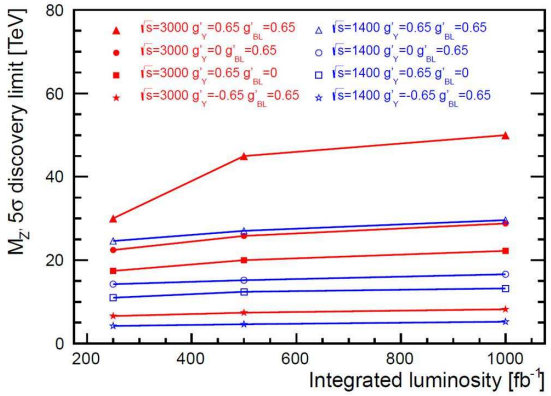

Figure 20: Expected 5σ discovery limit for Z' mass from measurement of $e^+e^- \to \mu^+\mu^-$, given as a function of the integrated luminosity.

4.4 Complementarities with the LHC program

In this section we would like to emphasize a necessity of building a lepton collider, in this case CLIC, as a precision tool to complement the experimental program of the LHC and its high-luminosity extension, HL-LHC. This comes from the fact that the relatively clean environment of e^+e^- collisions is maintained even at the highest energy, while at HL-LHC the increase of the instantaneous luminosity results in pile-up of $\sim$200 events (pile-up of $\sim$60 is expected already at 14 TeV LHC Phase 2 [20]),

deteriorating experimental conditions despite the increase of statistics. Several examples are given below where estimated ATLAS results [25] are taken to illustrate the HL-LHC potential.

At CLIC, most of the Higgs couplings can be determined with a sub-percent statistical uncertainty (as shown in [9]), while at HL-LHC the corresponding uncertainties are of the order of 5-20% [25]. Percent-level precision may be necessary to distinguish the light Higgs boson of an extended theory from a Standard Model Higgs boson. In addition, at an e^+e^- collider, the Higgsstrahlung production mechanism enables model-independent determination of the Higgs properties.

The CLIC capabilities to address beyond the Standard Model physics are also illustrated in Figure 19, where the single and double Higgs production at 3 TeV center-of-mass energies enables to probe the Higgs compositeness scale up to 70 TeV. At HL-LHC, depending on the model of compositeness, a scale of several TeV can be reached [15].

In addition, to study new particles directly, CLIC provides sensitivity to BSM physics through the precision measurements of sensitive observables, where, for example, Z' boson mass can be probed with 5σ confidence level up to a mass scale of 50 TeV (Figure 20), while the HL-LHC (ATLAS) can reach only $\approx$8 TeV with 3000 fb^{-1} of data (Figure 21 [25]).

Furthermore, high-energy CLIC operation allows measuring of the Higgs trilinear self-coupling parameter λ at $\approx$10% level, what would be probably difficult to reach at HL-LHC, where e.g. only 8.4 signal events are expected in the cleanest $HH \to b\bar{b}\gamma\gamma$ double-Higgs decay channel [25].

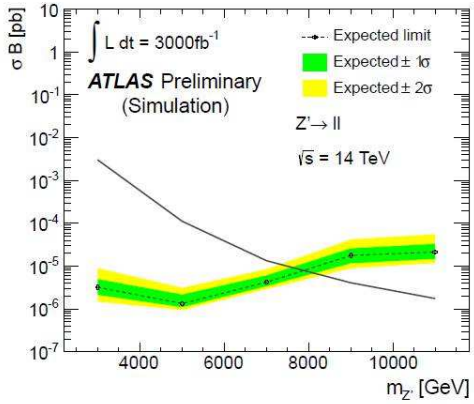

Figure 21: Expected 1σ and 2σ sigma HL-LHC ATLAS sensitivity to Z' mass scale.

Concerning BSM, CLIC would be able to measure masses of pair-produced gauginos, sleptons and heavy Higgs bosons with $O(1\%)$ precision, with sensitivity extending up to the kinematic mass limit of 1.5 TeV, what complements the HL-LHC program to measure heavier supersymmetric partners (Figure 22 [25]).

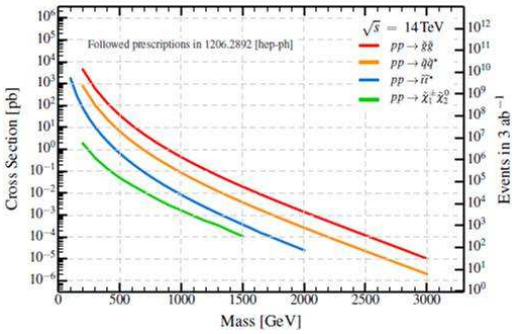

Figure 22: Illustration of HL-LHC capability to probe SUSY processes. Cross-sections are given versus the kinematic mass scale.

5 Summary and conclusion

The CLIC accelerator is an attractive option of a future e^+e^- collider, with the feasibility demonstrated through the extensive simulation and prototyping, accelerator and detector R&D. Staged implementation offers a broad physics program, from precision studies of the Higgs sector to BSM probes. Most of the Higgs couplings can be probed at a percent or sub-percent level, with the Higgs production via Higgsstrahlung enabling model-independent extraction. Rare decays can be accessed with a statistical precision of several percent, and the Higgs self-coupling to $\leq$12%. Composite Higgs can be indirectly probed up to the compositness scale of 70 TeV. Scan of the top mass threshold allows for top mass determination with a statistical uncertainty smaller than the theoretical one. Employment of the beam polarization enables determination of the top Yukawa coupling below 4%. Beyond the Standard Model physics can be accessed through direct and indirect searches. Direct observation of SUSY particles production allows for determination of their masses at a percent level, in most of the available scenarios, while the indirect searches extend the energy scale far beyond the kinematic reach of the machine (as in the case of the extended gauge theories).

The foreseen physics program at CLIC extends and complements the physics studies planned for LHC and HL-LHC, providing research opportunities at the forefront of particle physics for several decades.

Acknowledgments

The Vinca Institute activity at CLIC/CLICdp has been supported by the Ministry of Education, Science and Technological Development of the Republic of Serbia, through the project OI171012. The author is in debt to colleagues from the CLICdp collaboration, providing update on ongoing physics studies.

[1] L. Linssen et al. (editors), Physics and Detectors at CLIC: CLIC Conceptual Design Report, CERN-2012-003, CERN, 2012.

[2] M. Aicheler et al., A Multi-TeV Linear Collider based on CLIC Technology, CLIC Conceptual Design Report, CERN-2012-007, 2012.

[3] M. A. Thomson, Particle Flow Calorimetry and the PandoraPFA Algorithm, Nucl. Instrum. Methods, A611 (2009) 25, arXiv:0907.3577.

[4] S. Lukic, I. Bozovic Jelisavcic, M. Pandurovic, I. Smiljanic, JINST **8** P05008, (2013).

[5] H. Aihara et al. (editors), SiD Letter of Intent, SLAC-R-989, Fermilab-LOI-2009-01, Fermilab-Pub-09-681-E, 2009.

[6] T. Abe et al., The International Large Detector: Letter of Intent, Fermilab-LOI-2010-03, Fermilab-Pub-09-682-E, DESY-09-87, KEK-Report-2009-6, 2010.

[7] M. Frank, A Detector Description Toolkit for High Energy Physics Experiments, Users Manual, http://frankm.web.cern.ch/frankm/DD4hep/DD4hep Manual.pdf

[8] N. Nikiforou [on behalf of the CLICdp Collaboration], The New CLIC Detector Simulation Model, LCWS 15, 02-06 November 2015, Whistler, Canada.

[9] H. Abramowicz et al. [CLICdp Collaboration], Physics at the CLIC e^+e^- Linear Collider Input to the Snowmass Process 2013, 2013, arXiv:1307.5288.

[10] P. Lebrun et al. (editors), The CLIC Programme: towards a staged e^+e^- Linear Collider exploring the Terascale, CERN, 2012, ANL-HEP-TR-12-51, CERN-2012-005, KEK Report 2012-2, MPP-2012-115, https://edms.cern.ch /document/1234246/.

[11] ATLAS Collaboration, Observation of a new particle in the search for the Standard Model Higgs boson with the ATLAS detector at the LHC, Phys. Lett. B716 (2012) 1.

[12] CMS Collaboration, Observation of a new boson at a mass of 125 GeV with the CMS experiment at the LHC, Phys. Lett. B716 (2012) 30.

[13] S. Redford [on behalf of the CLICdp Collaboration], Higgs and BSM physics at CLIC, European Physical Society Conference on High Energy Physics 2015, 22-29 July 2015, Viena, Austria, CLICdp-Conf-2015-007.

[14] M. A. Thomson, Model-independent measurement of the $e^+e^- \to HZ$ cross section at a future e^+e^- linear collider using hadronic Z decays, Eur. Phys. J. C76 (2016) 72.

[15] G. Milutinovic-Dumbelovic, I. Bozovic-Jelisavcic, C. Grefe, G. Kacarevic, S. Lukic, M. Pandurovic, P. Roloff, I. Smiljanic, Physics potential for the measurement of $\sigma(H\nu_e\bar{\nu}_e) \times BR(H \to \mu^+\mu^-)$ at the 1.4 TeV CLIC collider, Eur. Phys. J. C75, (2015) 515.

[16] C. Grefe, E. Sicking [on behalf of the CLICdp Collaboration], $H \to \gamma\gamma$ and $H \to Z\gamma$ at CLIC with $\sqrt{s}$ =1.4 TeV, Americas Workshop on Linear Colliders 2014, Fermilab.

[17] I. Bozovic-Jelisavcic [on behalf of the CLICdp Collaboration], CLIC physics overview, 17th Lomonosov Conference on Elementary Particle Physics, Moscow State University, Moscow, 20-26 August, 2015, http://www.icas.ru/english/LomCon/17lomcon/17lomcon_programme.htm, CLICdp-Conf-2016-001.

[18] V. Khachatryan et al. (CMS Collaboration), Measurement of the top quark mass using proton-proton data at $\sqrt{(s)}$=7 and 8 TeV, Phys. Rev. D93 (2016) 072004.

[19] K. Seidel, F. Simon, M. Tesar, S. Poss, Top quark mass measurements at and above threshold at CLIC, Eur. Phys. J. C 73 (2013) 2530.

[20] M. Klute [on behalf of the ATLAS and CMS collaborations], Highlights of LHC Run I and first 13 TeV results, LCWS15 6-10 November, Whistler, Canada, http://agenda.linearcollider.org/event/6662/session/0/contribution/82/material/slides/0.pdf.

[21] M. Battaglia, J-J. Blaising, J. S. Marshall, S. Poss, M. Thomson, A. Sailer, E. van der Kraaij, Physics performance for Scalar Electron, Scalar Muon and Scalar Neutrino searches at $\sqrt{s}$ =3 TeV and 1.4 TeV at CLIC, JHEP 1309 (2013) 001.

[22] T. Barklow, A. Munnich and P. Roloff, Measurement of chargino and neutralino pair production at CLIC, 2011, CERN LCD-Note-2011-037.

[23] R. Contino, C. Grojeanb, D. Pappadopulo, R. Rattazzi and A. Thamm, Strong Higgs Interactions at a Linear Collider, JHEP 1402 (2014) 006.

[24] J-J. Blaising, J.D. Wells, Physics performances for Z' searches at 3 TeV and 1.5 TeV CLIC, arXiv:1208.1148.

[25] P. Glaysher, Search for New Phenomena at the High-Luminosity LHC with ATLAS, Proceedings of the 17th Lomonosov Conference on Elementary Particle Physics, August 20-26, 2015, Moscow, Russia, http://www.icas.ru/english/LomCon/17lomcon/17lomcon_programme.htm.